Towards sustainable polymeric nano-carriers and surfactants: facile low temperature enzymatic synthesis of bio-based amphiphilic copolymers in $scCO_2$

S. Curia, S.M. Howdle*

University of Nottingham, School of Chemistry, University Park, Nottingham, NG72RD, UK

Corresponding author: Tel.: +44 (0)115 951 3486; fax: +44 (0)115 846 8459; email: Steve.Howdle@nottingham.ac.uk

We demonstrate that useful bio-based amphiphilic polymers can be produced enzymatically at a mild temperature, in a solvent-free system and using renewably sourced monomers, by exploiting the unique properties of supercritical CO_2 ($scCO_2$). We present the use of a novel near-ambient temperature approach to prepare renewable amphiphilic ABA copolymers in $scCO_2$. Bio-based commercially available monomers have been polymerised to prepare chains with targeted molecular weight. The amphiphilic materials were prepared by end-capping the synthesised polymers with methoxy poly(ethylene glycol) (MPEG) chains in a one-pot high pressure reaction utilising *Candida Antarctica Lipase B* (CaLB) as a catalyst at a temperature as low as 35 °C.

The block copolymers are characterised by ^{1}H-NMR, GPC and DSC in order to carefully assess their structural and thermal properties. These polymers form self-assembled aggregates in aqueous environment and these nanostructures are studied through DLS, TEM and UV-Vis. Highly hydrophobic Coumarin-6 was used as a model to prove dispersion in water of lipophilic molecules. Maximum bubble pressure tests demonstrate the reduction in surface tension of these polymers and comparisons are made directly to commercial polymeric non-ionic surfactants.

1 Introduction

The large-scale production of amphiphilic block copolymers began in the 1950s, and these interesting macromolecules continue to attract considerable attention.[1-5] Amphiphilic block

copolymers form nanostructures (*e.g.* micelles and vesicles) that can find application as drug encapsulation and delivery systems and also in formulations as wetting agents, compatibilisers, emulsifiers and detergents.[1-3, 5-14] For example, polymeric micelles are characterised by a core-shell structure and have emerged as potential carriers for highly hydrophobic molecules because these can be encapsulated in the lipophilic core of the micelles.[1, 11] Polymeric vesicles (or polymersomes) are hollow spherical aggregates that contain an aqueous environment in the core surrounded by a bi-layer membrane. The core of the polymersome can be utilised to encapsulate hydrophilic molecules, whilst the membrane can contain lipophilic molecules within its hydrophobic core.[14]

The hydrophilic segment of amphiphilic copolymers is responsible for stabilisation of the self-assembled nanostructures in aqueous environments and is normally made of poly(ethylene glycol) (PEG),[1, 4, 5, 10, 15] which has many advantages, such as high hydrophilicity, flexibility and biocompatibility.[15] In addition to this, in recent years green routes for the production of bio-based PEGs have been reported.[16, 17] Thus, making this polymer not only a safe and biocompatible material but also a green and sustainable choice.[18, 19] Furthermore, PEGs with molecular weight lower than 4000 g mol^{-1} were found to be biodegraded by many bacteria so they do not accumulate in the environment.[20]

The hydrophobic segment is made of lipophilic polymers, such as poly(propylene glycol) (PPG), and multiblock copolymers containing PPG and PEG (commercially known as Pluronics®) can spontaneously organise in micelles and, hence, have been widely investigated for medical applications.[3] Nonetheless, Pluronics display slow biodegradability under physiological conditions and they can accumulate in the body.[21] For this reason, an important prerequisite for a non-degradable or poorly degradable polymer, to be used as a drug carrier, is a molecular weight sufficiently low to allow for excretion *via* the renal route.[22] Furthermore, Pluronics are generally characterised by a fairly high (0.01-10% wt) critical aggregation concentration (CAC) due to the weak hydrophobicity of the PPG block: this means that the nanostructures are highly unstable and the micelles are likely to dissociate upon dilution (*i.e.* after injection in the body).[1, 21] On the contrary, a low CAC ensures that the self-assembled structure is retained in the bloodstream.

For these reasons, biodegradable polyesters such as poly(lactic acid) (PLA) and poly(caprolactone) (PCL) have been investigated extensively as hydrophobic segments in combination with PEG for the preparation of amphiphilic polymers that can be more easily eliminated from the body. These materials also show a higher CAC as a result of the increased hydrophobicity of PLA and PCL compared to that of PPG.[4, 6, 9, 15, 21] Moreover, the incorporation of a hydrolytically degradable block in the structure ensures a faster elimination from the body upon degradation of the polyester segment.[21]

To sum up, the ideal amphiphilic copolymer, to satisfy societal need for drug delivery and medical applications through to detergents and surfactants for home and personal care, must meet specific fundamental requirements. In particular, low toxicity, biodegradability and biocompatibility, whilst also having the desired amphiphilic characteristics and an appropriate CAC.

In addition to all these needs, there has been an increasing focus on sustainable synthetic approaches and the use renewable raw materials. This arises not only from future supply constraints for fossil-base resources, but also as a response to a strong market and customer demand to increase the overall sustainability of materials and processes and to lower carbon footprint.[5]

There is no doubt that the use of green monomers to replace non-renewable and fossil-based raw materials is an important research focus of modern polymer science, both in academia and industry.[23, 24] Naturally occurring and bio-derived molecules are fundamental resources that can be employed to achieve a more sustainable plastic industry and lead to polymers that are intrinsically biodegradable (*e.g.* polyesters).[24]

Another important focus of modern polymer chemistry is the replacement of organic solvents with greener alternatives, and the design of new sustainable synthetic processes.[19, 25] In recent years interest in the use of compressed CO_2 as a reaction medium or plasticiser for polymer synthesis and processing has increased.[26-29] High-pressure CO_2 has been exploited as a solvent for polymerisations,[30, 31] as a foaming agent,[26, 32] for precipitation/separation,[33] particle formation[34, 35] and encapsulation.[36]

$ScCO_2$ is a poor solvent for most of the polymers (with rare exceptions, such as fluoro-polymers, silicones and few vinyl esters polymers/copolymers),[28, 31] but by contrast is very effective at penetrating and dissolving into polymeric materials; plasticising and effectively liquefying many polymers at temperatures well below their normal ambient pressure glass transition temperature (T_g) and melting point (T_m).[35, 37-40] This has opened up a range of new approaches to green polymerisation.

Under normal pressure conditions, polycondensations and melt-polymerisations require high temperatures (normally greater than 160 °C for polycondensations) to work effectively.[41-45] The higher temperatures are normally required in order to lower the viscosity of the growing polymeric materials and to activate the conventional catalysts. By necessity metal-based catalysts are used that are potentially toxic[46-48] and expensive. Enzymes could not normally function effectively at temperatures higher than 100 °C. For instance, the activity of the lipase CaLB is vastly reduced above 90 °C.[49, 50]

We previously exploited $scCO_2$ to prepare a range of green functional materials with targeted degree of polymerisation (DP) through enzymatic syntheses at near-room-temperature conditions and without pre-modification of the monomers.[51]

In this paper we synthesise specific end-functionalised novel green amphiphilic copolymers based on azelaic acid, 1,6-hexanediol and PEG in $scCO_2$ (Figure 1). Azelaic acid is a naturally occurring saturated dicarboxylic acid with antibacterial and anti-inflammatory properties.[52, 53] Azelaic acid shows a small solubility in $scCO_2$ and is characterised by a high T_m (~110 °C).[54] It is found in wheat, rye and barley,[55] but it can also be produced through ozonolysis of oleic acid.[54, 56] This diacid is not soluble in apolar solvents, and hence normally requires end-group modification to form the ester to convey solubility, lower the T_m, and allow for further processing. In fact, the only polymerisations shown in the literature of this diacid were performed in the melt with the aid of metal catalysts at temperatures as high as 230 °C.[57, 58]

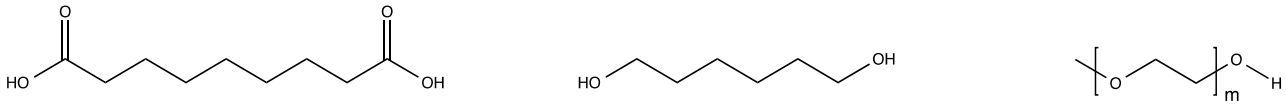

Figure 1 - Azelaic acid, 1,6-hexanediol and methoxy poly(ethylene glycol) have been used as building blocks for the preparation of amphiphilic polyesters.

However, because of its unusual properties and availability from renewable sources, azelaic acid could represent an important building block for the design of amphiphilic polymeric materials and other applications. Therefore, we have exploited the use of $scCO_2$ to allow low temperature enzymatic polycondensations, without pre-modification of the diacid, with a renewable diol,[59-61] and targeting the molecular weight of the chains by using end-cappers of methoxy poly(ethylene glycol) (MPEG) with two different molecular weight (350 and 550 g mol^{-1} respectively).

Amphiphilic copolymers were prepared directly from the diacid and characterised through ^{1}H and ^{13}C NMR and differential scanning calorimetry (DSC) to assess the structural and thermal properties. Their self-assembly in water was investigated through dynamic light scattering (DLS), transmission electron microscopy (TEM) and ultraviolet-visible spectroscopy (UV-Vis) showing that the polymer can form nanostructured aggregates and the properties can be tuned carefully by choosing the length of the hydrophilic and hydrophobic segments.

2 Experimental

2.1 Materials

Azelaic acid (98%) was purchased from Alfa Aesar (UK) and dried for 24 h under vacuum (100 mbar) at 50 °C before use; 1,6-hexanediol (97%) was purchased from Sigma Aldrich (UK) and dried at RT for 24 h under vacuum (100 mbar) before use. MPEG550 (M_n~550 g mol^{-1}) and MPEG350 (M_n~350 g mol^{-1}) were purchased from Sigma Aldrich (UK) and stored over fresh molecular sieves (4Å, particle size 1.6-2.5 mm). Tween® 20 (PEG sorbitan monolaurate, M_n~1200 g mol^{-1}) and Pluronic® L-121 (PEG-*b*-PPG-*b*-PEG, M_n~4500 g mol^{-1}) were used as received. Coumarin-6 (98%) and 1,6-diphenyl-1,3,5-hexatriene (98%) were purchased from Sigma Aldrich (UK) stored in the dark and used as received.

Novozym 435 (CaLB immobilised on cross-linked acrylic resin beads) was kindly donated by Novozymes (Denmark) stored at 4 °C and dried for 24 h under vacuum (100 mbar) at room temperature (RT) before use. All the solvents were of analytical grade, or Chromasolv® were specified, purchased from Sigma Aldrich (UK) and used as received. Millipore water (18.2 MΩ.cm, <5 ppb TOC) dispensed through a 0.22 μm filter was used for the preparation of all the polymer dispersions in water.

Supercritical Fluid Chromatography (SFC) grade 4.0 CO_2 (minimum purity 99.99%) was purchased from BOC Special Gases (UK) and used as received.

2.2 Methods

Enzymatic synthesis MPEG-b-PHAz-b-MPEG. In a typical procedure the diacid (3.40 mmol, 640 mg), diol (DP6: 2.91 mmol, 344 mg; DP3: 2.55 mmol, 301 mg) and MPEG550 or MPEG350 (DP6: 0.97 mmol, 534 mg ; DP3: 1.70 mmol, 935 mg) were added to the stainless steel reaction autoclave (20 mL),[29, 31] along with enzyme and fresh molecular sieves (3 Å, particle size 1.6-2.5 nm) (10% by weight of enzyme beads and 25% of molecular sieves relative to the total amount of monomers and MPEG). An excess of diacid was used to ensure the synthesis of diacid terminated PHAz blocks (since the MPEG chains can react only with the carboxylic acid moieties). The vessel was then sealed and pressurised up to 50 bar. The temperature was then raised to 35 °C, the pressure

stabilised at 275 bar and the reaction left to run for 24 h while stirring at 100 rpm. To avoid polymer foaming and consequent tubing blockages,[62] the reactions were stopped by cooling the vessel in a water/ice bath (0 °C) and the CO_2 was vented when the pressure went below 20 bar. Finally, the product was dissolved in 6 mL of toluene (gently heating at 40 °C to melt any residual unreacted 1,6-hexanediol and, thus, retain information on conversion) and filtered to remove the enzyme and sieves. Filtered solutions were dried at 40 °C under reduced pressure leaving white solid-waxy polymeric products. Product yield was calculated dividing the dry product mass by the theoretical mass (^{1}H-NMR analyses showed that the amount of unreacted species was negligible).[63-65]

The nomenclature used in this paper is detailed in (**Table 1**).

Table 1 – Nomenclature and letter scheme of the ABA copolymers presented in this study. The variables are the length of the MPEG block used for end-capping and the targeted molecular weight of the PHAz synthesised during the enzymatic polymerisation.

	Structure	M_n^{MPEG} (g mol^{-1})[a]	M_n^{PHAz} (g mol^{-1})[b]
(a)	$MPEG_{12}$-$PHAz_3$-$MPEG_{12}$	550	967
(b)	$MPEG_{12}$-$PHAz_6$-$MPEG_{12}$	550	1778
(c)	$MPEG_7$-$PHAz_3$-$MPEG_7$	350	967
(d)	$MPEG_7$-$PHAz_6$-$MPEG_7$	350	1778

[a]Declared by supplier; [b]Theoretical targeted M_n.

The reaction scheme is shown below (**Figure 2**).

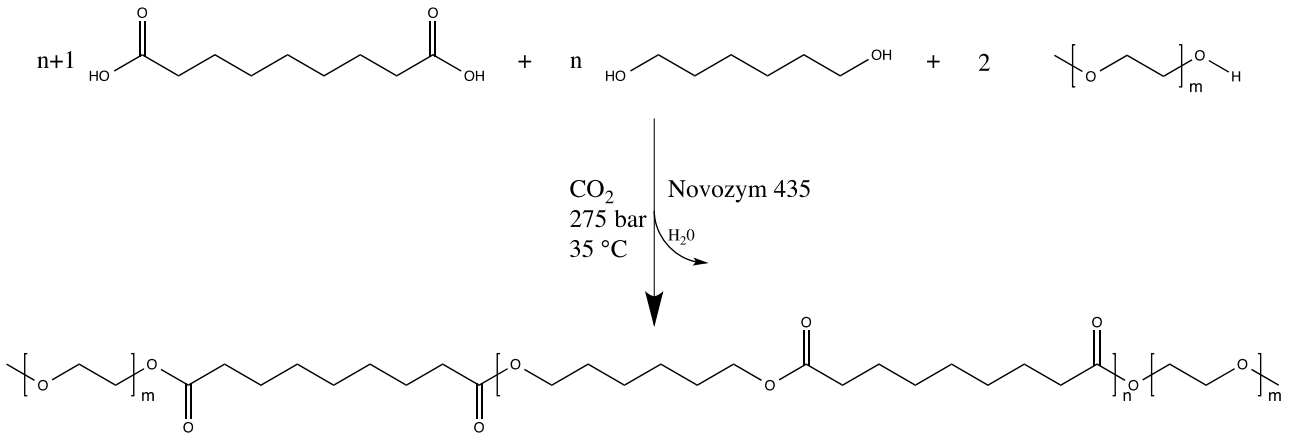

Figure 2 – Lipase-catalysed synthesis from azelaic acid, 1,6-hexandiol and MPEG to MPEG-*b*-PHAz-*b*-MPEG in $scCO_2$. An excess of azelaic acid was used in order to obtain an ABA-type block copolymer (since the MPEG chains are able to react only with the diacid moieties).

^{1}H and ^{13}C-NMR analysis. NMR analyses were conducted on a Bruker Avance III 500 spectrometer in $CDCl_3$ or D_2O (20 mg mL^{-1}). The number of scans was 16 for ^{1}H (500 MHz) and 4096 for ^{13}C (125 MHz). Conversion and chain length were analysed through monomer peak and end-group analysis. The chemical shifts were reported in part per million (ppm) with respect to residual solvent peaks (7.26 ppm for ^{1}H and 77.36 ppm for ^{13}C in $CDCl_3$, 4.80 ppm for ^{1}H in D_2O).[66]

Gel permeation chromatography (GPC). The molecular weight distributions of the samples were analysed using a Polymer Laboratories GPC 50 with a refractive index detector and calibrated with poly(styrene) standards in the range of 100 g mol^{-1} – 500 kg mol^{-1} (poly(styrene) standards were chosen for the good agreement with the results obtained by ^{1}H-NMR). The machine was equipped with a PL PLgel guard (8μm) column followed by two PL PLgel Mixed-D (8 μm) columns. The samples were run in $CHCl_3$ Chromasolv® (5 mg mL^{-1}) at a flow rate of 1 mL min^{-1}. Cirrus software was used for analysis.

Differential scanning calorimetry (DSC). DSC analyses were performed using a TA Instruments (USA) TA-Q2000 DSC calibrated with sapphire and indium standards. In a standard experiment, the sample (2.00 ± 0.10 mg) was melted with a first heating scan up to 100 °C (10 °C min^{-1}) and cooled down to -90 °C (10 °C min^{-1}). A second heating scan up to 100 °C, with the same heating rate, was then carried out to detect the melting point. Isothermal 5-minute segments were performed at the conclusion of each ramp. The experiments were carried out under a N_2 flow (50 mL min^{-1}). The T_m was taken as the maximum of the endothermic peak. Each experiment was repeated three times (on three different portions of the sample) and the results are shown as the average ± 1 standard deviation.

Preparation of polymer nanoparticles. The polymeric nanostructures were prepared through nanoprecipitation from THF Chromasolv®. The appropriate amount of polymer was dissolved in THF (1 mL) and this solution was added dropwise (100 μL, 30 seconds) to water (4 mL) whilst stirring at 1500 rpm. The THF was left to evaporate for 1 hour whilst stirring at ambient pressure, and then under reduced pressure (75 mbar) for 30 minutes at room temperature.

Dynamic light scattering (DLS). DLS analyses were performed using a Malvern Zetasizer Nano ZS system in order to determine the hydrodynamic diameter of the polymeric particles in water. Polystyrene disposable cuvettes were used and the samples were not filtered to retain information on the possible presence of microscopic aggregates. The analyses were performed at 25 °C on a 1

mL sample collecting the scattered light at 173°. Typically, three separate experiments of 10-15 runs (chosen by the instrument depending on the optical quality of the dispersions) were performed for each sample to check upon data significance and reliability.
For the size-temperature study, 5 minutes were allowed after each temperature step in order for the sample to reach thermal equilibrium before collection of the data.

Transmission electron microscopy (TEM). TEM analyses were carried out to obtain a visual observation of the nanostructures on a JEOL 2000-FX microscope. Typically, 30 µL of the polymer dispersions (0.10% in water) was dropped on holey carbon coated TEM grids (EMResolutions, UK). After drying of the water, 15 µL of 1% by weight aqueous uranyl acetate (UA) solution were added to each grid and dried with filter paper after 1 minute to obtain negative background staining. Before addition, the UA solution was passed through a 0.22 µm filter to remove any UA acetate crystals from the solution.

Coumarin-6 (C6) incorporation. The incorporation of C6 has been studied to test the ability of the polymers to act as nanocarriers for the encapsulation and stabilisation of hydrophobic molecules in water. To ensure the presence of one phase in the polymer/C6 solution, dichloromethane (DCM) was used as a solvent for the nanoprecipitation. A stock solution of C6 dissolved in DCM (2.5% w/v) was prepared and 50 µL of this solution was added to 500 µL of a DCM 2% w/v polymer solution. This final solution (550 µL) was added dropwise (110 µL, 30 seconds) to 10 mL of water whilst stirring at 1500 rpm obtaining a final solution 0.1% wt of polymer in water. The DCM was left to evaporate for 1 hour while stirring at ambient pressure, and then under reduced pressure (75 mbar) for 30 minutes at room temperature. The solutions were filtered through membrane syringe filter (0.22 µm, Millex.LG, Millipore Co., USA) to exclude larger aggregates and undissolved C6. Aliquots of the filtered solutions were used for UV-Vis analyses (at 25 °C) to quantify the amount of C6 dispersed by each polymer.

UV-Vis quantification of C6 incorporation. The ability of the synthesised polymers to act as systems to encapsulate C6 was determined through UV-Vis in THF using a Perkin Elmer Lambda 25 spectrometer with a matched pair of Hellma® 6030-UV quartz cuvettes (pathlength 10.00±0.05 mm). For a typical experiment, 0.3 mL of polymer dispersion in water with incorporated C6 (prepared as described previously) were added to 2.7 mL of THF. The absorption was recorded between 550 and 350 nm (480 nm min^{-1}, slit width 1 nm, data interval 1 nm).

The amount of dispersed C6 for each polymer sample was determined through comparison with the absorbance of standard solutions of C6 in 9:1 THF:water with known concentration (y=70.1x; R^2>0.99) considering the absorbance value at 452 nm. Each experiment was run in duplicate to check upon reproducibility.

Critical aggregation concentration (CAC) determination. The CAC of the synthesised polymers was determined through UV-Vis in water using a Perkin Elmer Lambda 25 spectrometer with a matched pair of Hellma® 6030-UV quartz cuvettes (pathlength 10.00±0.05 mm) at 25 °C. Aqueous dispersions with different concentrations (typically from 0.1% to 0.0001% wt) were prepared for each polymer using the nanoprecipitation methodology (from THF). A small aliquot of methanolic 1,6-diphenyl-1,3,5-hexatriene (DPH) (0.4 mM) was added to each polymer dispersion (10 µL mL^{-1}) and equilibrated overnight on a orbital shaker (400 rpm). The absorption spectra were recorded from 390 to 330 nm (480 nm min^{-1}, slit width 1 nm, data interval 1 nm). Dispersions with the same polymer concentration, but without DPH, were used as reference for each measure. Each experiment was run in duplicate to check reproducibility. Because of the cloudiness of some of the polymer dispersions at high content of polymer, 0.05% wt was the highest analysed concentration and some of the spectra were fairly noisy, due to the lower light intensity passing through both the reference and the sample (consistent background absorption). The CAC was determined by the two extrapolated lines of the absorbance at 362 nm at low and high concentration regions.[67]

Maximum bubble pressure test. The surface tension of the polymer dispersions in water (0.2% wt, 20 mL) was determined by using a SITA t100 Bubble Pressure tensiometer. The MPEG-PHAz-MPEG copolymers were compared to two commercial surfactants (Tween 20 and Pluronic L121). A sample containing only water was analysed as a control. The tests were run at 20 °C.

3 Results and discussion

3.1 Copolymers synthesis and characterisation

Azelaic acid is a commercially available bio-based monomer with antibacterial and anti-inflammatory properties,[52, 53] which we have exploited for green polyester synthesis using an enzyme and $scCO_2$ at near-ambient temperature (35 °C). The polymers were prepared in one pot by

adding together the monomers and end-cappers, with enzyme supported on cross-linked acrylic beads into the reaction autoclave. The reactions targeted specific the molecular weights by carefully controlling monomer and end-capper feed ratios. Once the autoclave was vented, yellowish waxy products were collected. After separation of the enzyme/molecular sieves and drying, light yellow/white waxy polymers were obtained in very good yields (Table 2).

Table 2 - Molecular weight distribution (from NMR and GPC), isolated yield and conversion of the synthesised MPEG-PHAz-MPEG copolymers.

Product	M_n^{th} (g mol^{-1})[a]	M_n^{NMR} (g mol^{-1})[b]	M_n^{GPC} (g mol^{-1})	$Đ$	ABA structure (%)[c]	Yield (%)[d]
(a) $MPEG_{12}$-$PHAz_3$-$MPEG_{12}$	2084	2500	2200	2.04	98	87
(b) $MPEG_{12}$-$PHAz_6$-$MPEG_{12}$	2896	3000	3200	2.24	93	84
(c) $MPEG_7$-$PHAz_3$-$MPEG_7$	1644	1800	1700	2.18	85	82
(d) $MPEG_7$-$PHAz_6$-$MPEG_7$	2455	2700	2400	1.83	93	91

[a]Calculated according to the reagents ratios; [b]Determined through ^{1}H-NMR from the ratio between the integrals of the peaks of the polymer backbone and the end-group peak; [c]Percentage of polymer with ABA structure determined through ^{1}H-NMR analyses (peak at 4.22 ppm); [d]Yield= weight of collected product/theoretical weight.

Exact conversions could not be estimated due to overlap of the peak assigned to the protons adjacent the alcohol group (3.65 ppm) in the HD monomer and the -CH_2- peak of the MPEG backbone (3.64 ppm). However, from the value expected for the peak of the MPEG backbone, the conversion approached 90% for all the polymers.

As a general example, the ^{1}H-NMR spectrum of (a) $MPEG_{12}$-$PHAz_6$- $MPEG_{12}$ (Figure 3) shows integrals of the peaks at 3.38 ppm (terminal methoxy group in each of the MPEG blocks) and at 4.05, 2.28, 1.63 and 1.38-1.32 ppm (PHAz backbone protons) and these were used to calculate the mass average molecular weight (M_n^{NMR}). The results show a very good agreement with expected molecular weights, thus indicating successful controlled polymerisation (Table 2). Furthermore, the normalised ratio between the integrals of the peaks at 4.22 and 3.38 ppm indicates that 98% of the detected MPEG is attached to the PHAz backbone for this copolymer; similar results were observed also for the other copolymers (see ^{1}H-NMR in the SI; no correlation between the presence of free MPEG residues and aggregation or CAC was found, as shown later from DLS, TEM and UV-Vis studies). This shows a high yield of end-capping and thus an efficient polymerisation to form ABA block copolymers *via* an enzymatic low-temperature approach. It is important to remark that only for practical reasons dissolution in toluene was used to physically separate the enzyme beads from

the product at the end of the reaction; however, our group previously demonstrated that it is also possible to completely avoid the use of conventional solvents by exploiting the plasticising effects of CO_2 to separate the enzyme beads from the polymer product.[62]

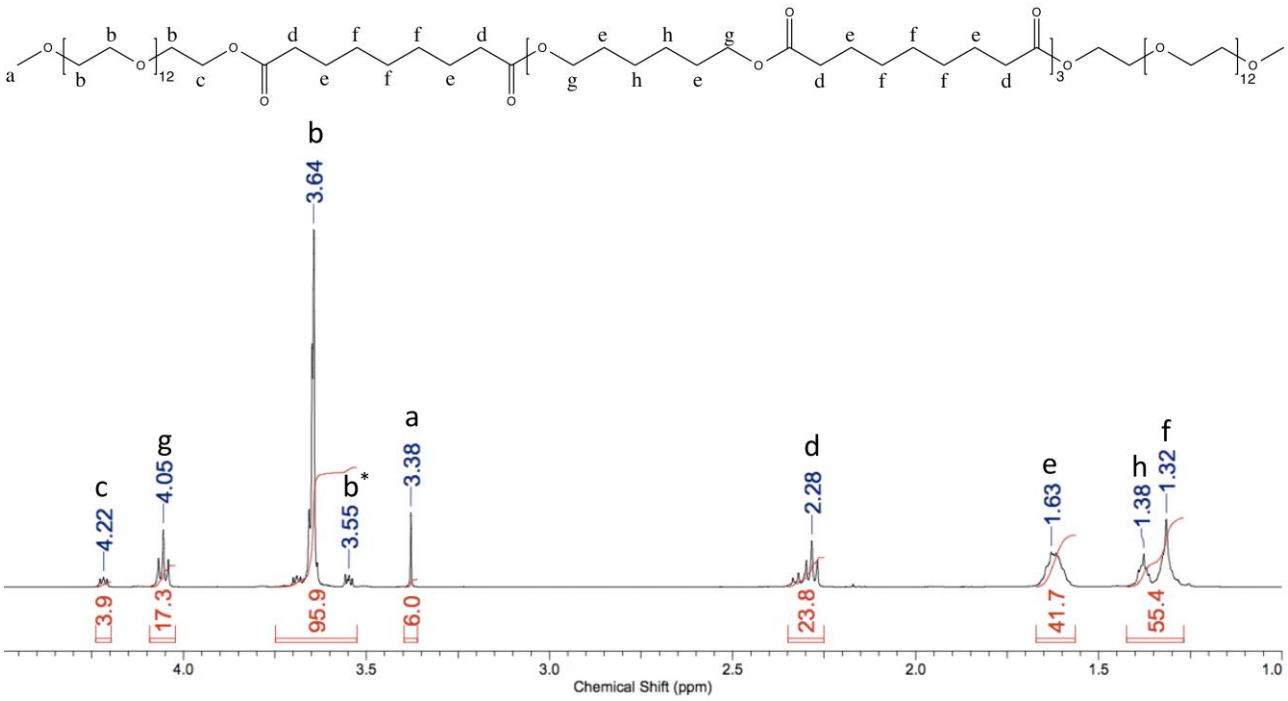

Figure 3 - ^{1}H-NMR of polymer (a) MPEG$_{12}$-PHAz$_3$-MPEG$_{12}$. Integrals of the peak at 3.38 ppm (terminal methoxy group) and 4.05, 2.28, 1.63 and 1.38-1.32 ppm (PHAz backbone) can be used to estimate the average molar mass of the polymer. The peak b (3.64 ppm) is assigned to the -CH$_2$- in the MPEG backbone, while the peak b* (3.55 ppm) is assigned to the -CH$_2$- protons directly attached to the terminal methoxy group (-O-CH$_3$).[8] ^{1}H-NMR spectra for the other copolymers are available in the SI.

To obtain additional information about molecular weight and dispersity, GPC measurements were performed with $CHCl_3$ as eluent and show good agreement with the molecular weights calculated by ^{1}H-NMR and predicted (Table 2). Furthermore, a dispersity value around 2 was found for all the polymers, as expected for linear polymers synthesised by polycondensation at high conversions.[64, 68] The obtained MPEG-PHAz-MPEG polymers were semicrystalline with low T_m (Table 3). Furthermore, two melting points could be identified for the copolymers (a) and (b), as expected for separate crystallisation of the polyester segment and the MPEG blocks that in this case were long enough to crystallise.[69, 70] Nonetheless, the higher T_m – attributed to the PHAz segment – was the bigger and sharper peak for all the polymers (see SI for DSC traces).

Table 3 – Thermal properties of the ABA copolymers obtained from DSC analyses (2nd heating scan). The values are shown as the average between 3 different measurements ± 1 standard deviation.

Product	T_m [a] (°C)	ΔH_m (kJ mol^{-1})[b]
(a) $MPEG_{12}$-$PHAz_3$-$MPEG_{12}$	32.9 ± 1.1	33.3 ±0.9
(b) $MPEG_{12}$-$PHAz_6$-$MPEG_{12}$	38.6 ±0.4	55.8 ±0.6
(c) $MPEG_7$-$PHAz_3$-$MPEG_7$	30.7 ±0.9	40.2 ±0.3
(d) $MPEG_7$-$PHAz_6$-$MPEG_7$	39.4 ±0.6	68.6 ±0.4

[a]Main T_m peak observed in the DSC trace

It is clear how a longer PHAz backbone (polymer (b) and (d)) results in a higher T_m and enthalpy of fusion (ΔH_m). This behaviour is attributed to larger crystallites that can be formed when longer polymer chains pack, and it has been observed for other polyesters at small molecular weight values.[71] The T_g could not be detected due to equipment limitations and high crystallinity of the copolymers, but it is expected to be around -60 °C as observed previously for similar polyesters.[72]

3.2 Aqueous self-assembly and surface tension studies

3.2.1 NMR studies

Effective aggregation in water, with a structure where the lipophilic block has restricted motion, was confirmed by comparison of ^{13}C-NMR spectra collected in D_2O and $CDCl_3$. Chloroform is a good solvent for the MPEG and PHAz blocks, while water is a good solvent only for PEG. For these reasons, in $CDCl_3$ the peaks of the MPEG and PHAz moieties are clearly observed, whereas in D_2O only the resonances attributed to PEG are detected (Figure 4). This implies that in $CDCl_3$ there is fast molecular motion of each block, while in D_2O the motion of the PHAz is restricted and, consequently, its resonances are collapsed and broadened.[7, 73] The same effect was also observed in the ^{1}H-NMR spectrum acquired in D_2O (see SI). Here again, the peaks attributed to the PHAz block are small and significantly broadened, clearly demonstrating that an aggregated structure with an external MPEG shell and an internal PHAz portion with restricted motion is formed in water (*e.g.* micelles, vesicles).[22]

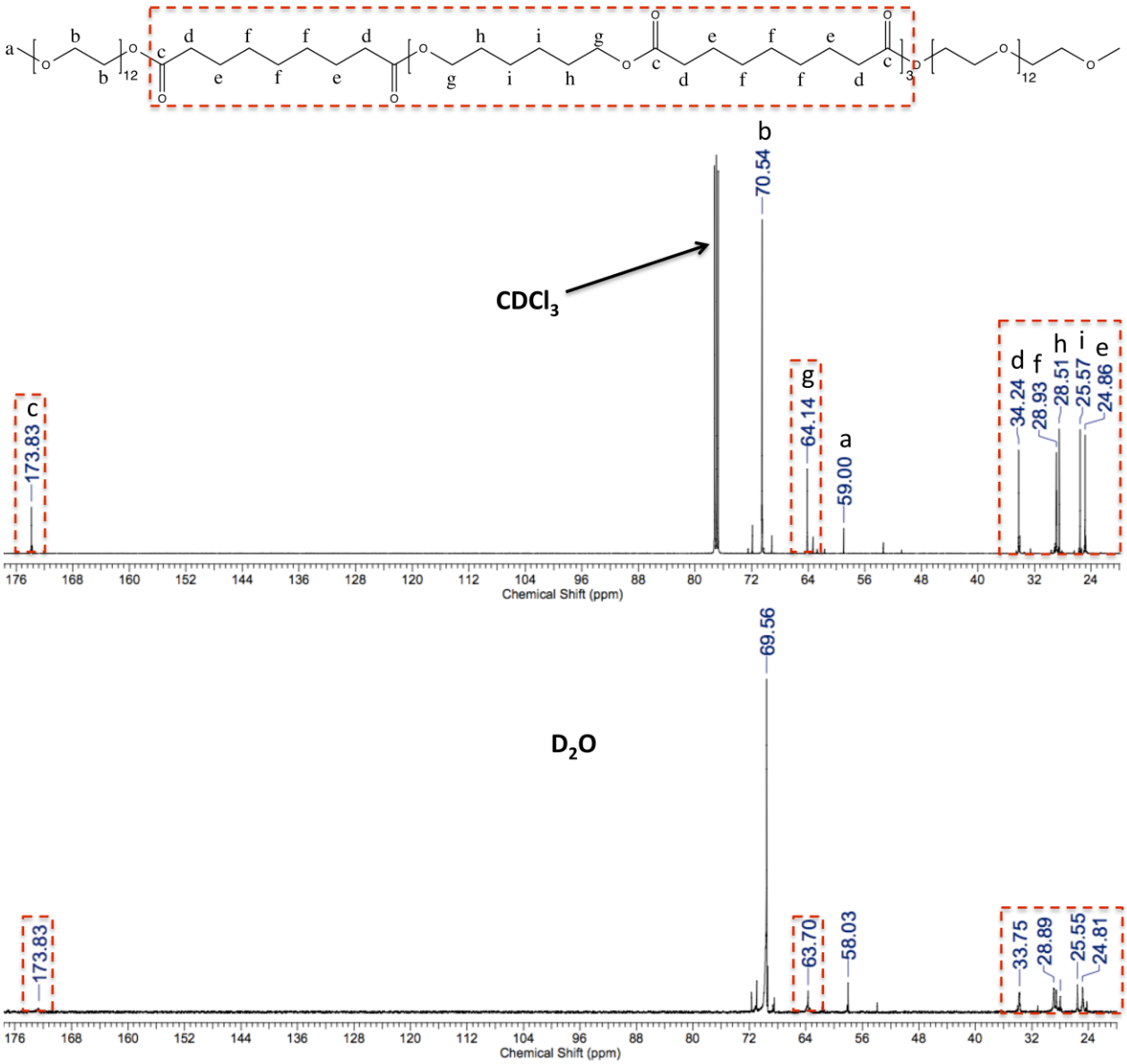

Figure 4 - ^{13}C-NMR spectra of (b) MPEG$_{12}$-PHAz$_6$-MPEG$_{12}$ in $CDCl_3$ (top) and D_2O (bottom) (20 mg mL^{-1}). All the peaks are clearly detected in chloroform, whilst the PHAz resonances (red dotted rectangles) are strongly suppressed in heavy water. In particular, the carbonyl peak (around 174 ppm) is almost undetectable in D_2O. This confirms the formation of aggregates with a rigid PHAz portion in aqueous environment.

3.2.2 DLS and TEM studies

In order to use a copolymer as a drug delivery vehicle or as an effective micellar system, it is essential to investigate the nature of its self-assembly in aqueous environment and determine the characteristic size of the self-assembled structures.

The nano-precipitation methodology has been previously shown as a successful way to prepare empty and drug/dye loaded polymeric particles.[2, 5] For this reason, we chose to use this method to prepare MPEG-PHAz-MPEG nanoparticles. In our process the desired amount of copolymer was

first dissolved in a non-selective water-miscible solvent (*i.e.* THF) and this solution was added dropwise to water while stirring, to allow for the THF excess to evaporate and the copolymers to assembly. Complete removal of the organic solvent was achieved by applying reduced pressure (75 mbar) at ambient temperature.

The diameter and size distribution of the structures formed was determined by DLS (Figure 5 upper). The DLS data for polymers (a), (c) and (d) displayed the presence of structures that are clearly quite large and likely indicate formation of aggregated structures or vesicles rather than spherical micelles.

To investigate this in more depth, TEM analyses (with negative background staining using uranyl acetate (UA)) were performed. The size determined through TEM analyses showed excellent agreement with the distribution by number obtained by DLS (Figure 5 lower). However, the DLS results were always slightly higher than the size observed in the TEM pictures, since they represent the hydrodynamic diameter of the solvated particles and those are necessarily bigger than the diameter of the dry aggregates observed through TEM. Furthermore, the intensity and size distribution obtained through DLS showed an overestimation of the dimension: because of the dependency on size of these type of distributions that leads to a size overestimation for non-monodisperse systems such as these polymeric nanoparticles (see SI for all the DLS distribution plots).

The TEM analyses confirmed the presence of spherical micelles for polymer (b), whilst the micrographs of polymers (a), (c) and (d) showed the presence of diverse structures. In more detail aggregated micelles and wormlike micelles could be identified for polymer (a) and (c), whilst aggregated micelles and possible vesicles were detected in polymer (d) (see SI for additional TEM micrographs), factors which may well also explain the larger sizes detected from DLS measurements.

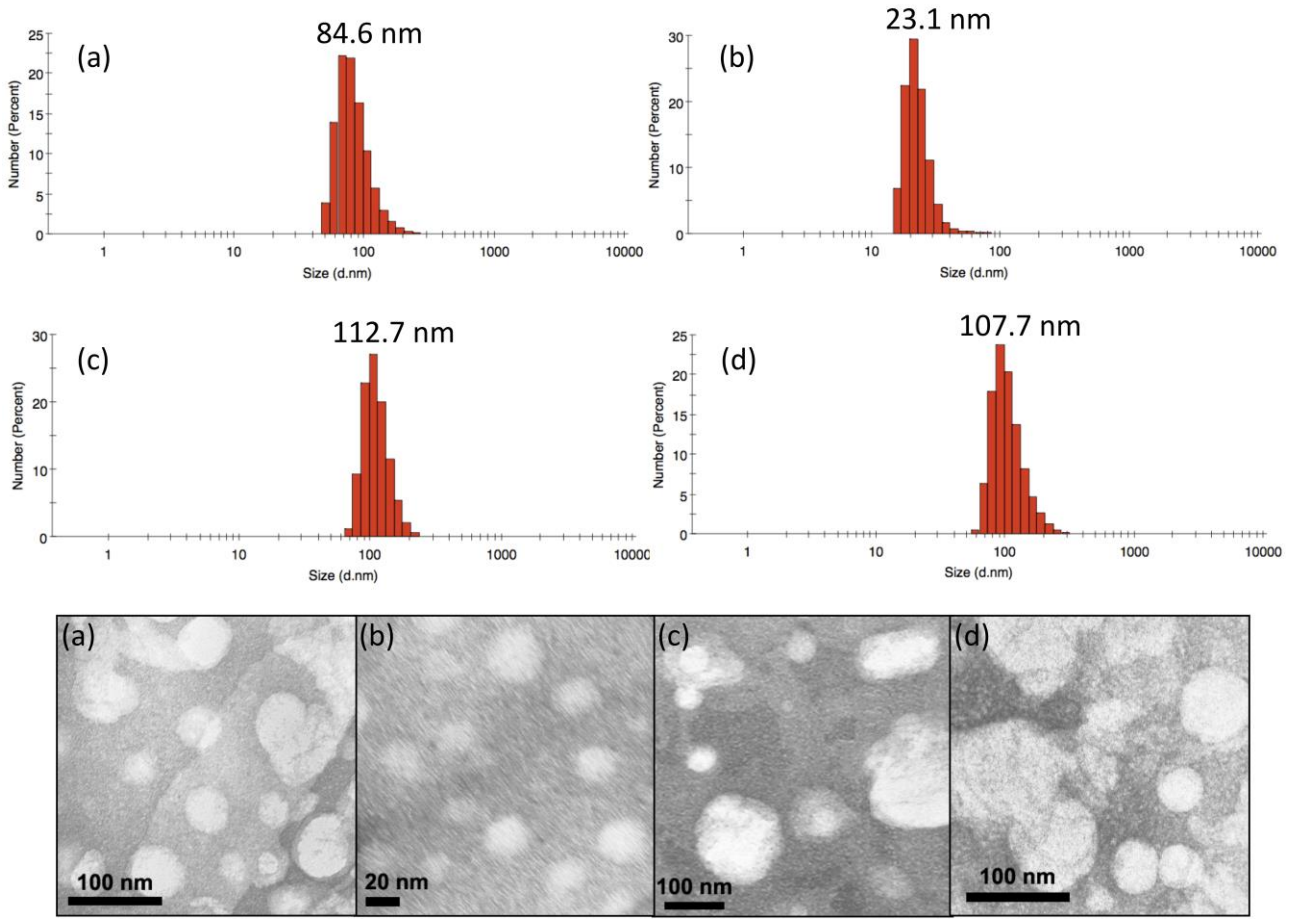

Figure 5 - Size distribution (by number) obtained through DLS analyses and TEM images of the copolymers (0.1% wt in water): (a) $MPEG_{12}$-$PHAz_3$-$MPEG_{12}$, (b) $MPEG_{12}$-$PHAz_6$-$MPEG_{12}$, (c) $MPEG_7$-$PHAz_3$-$MPEG_7$, (d) $MPEG_7$-$PHAz_3$-$MPEG_7$. The peak size is shown in each DLS plot. Discrete spherical micelles are observed for polymer (b). Images were taken with UA negative background staining.

It is well known that several parameters (such as the block-length ratio of the hydrophilic to the hydrophobic block, hydrophobicity of the apolar block, molecular weight *etc.*) influence the type and size of the nanostructure formed upon self-assembly. For instance, MPEG blocks with higher DP generally result in smaller micelles, as observed for other amphiphilic copolymers when increasing the size of the hydrophilic block.[2, 73] Short hydrophilic blocks can result in the formation of large structures upon hierarchical aggregation of smaller micelles.[74]

Furthermore, the length and crystallinity of the hydrophobic block (in this case the PHAz) can also influence the micellar size. For example, for PEG-PCL spherical micelles a smaller size was observed with increasing PCL molecular weight: this was attributed to the ability of the hydrophobic core to pack tightly in crystalline regions.[75] Besides, the degree of crystallinity of the core can also affect the morphology of the aggregates.[76] For instance, for a given PCL length a change in the crystallinity of the core of PEG-PCL block copolymers has been observed to shift the morphology from rods to spherical micelles.[77]

Therefore, in this case a particular balance between the PHAz core crystallinity and the PEG weight fraction might explain the formation of spherical micelles for polymer (b) and the different self-assembly/aggregation observed for the other copolymers. Further investigations are certainly required to understand thoroughly the self-assembly of these PHAz-based amphiphilic copolymers and unveil to role of the crystallinity, hydrophobic/hydrophilic ratio and interaction parameter of the PHAz block with water upon the aggregated nanostructures formed in aqueous environment.

Nonetheless these preliminary studies showed that all the copolymers formed self-assembled aggregates with sizes suitable for drug delivery, since nanoparticles smaller than 200 nm can avoid recognition from the reticuloendothelial system (RES).[75]

Structures with characteristic dimensions below 30 nm are highly desirable for pharmaceutical formulations.[2] Hence, the copolymer (b) $MPEG_{12}$-$PHAz_6$-$MPEG_{12}$ is particularly interesting, since this formed micelles with diameter around 20 nm. For this reason, the micellar size of this polymer was investigated further as a function of temperature (Figure 6).

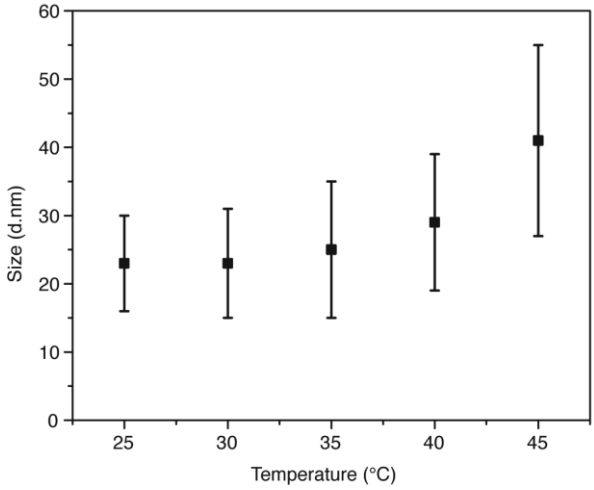

Figure 6 – Diameter of (b) $MPEG_{12}$-$PHAz_6$-$MPEG_{12}$ micelles *vs* temperature (0.1% wt in water). The size is stable between 25 and 35 °C. A significant increase of the peak value is observed at 45 °C. The size showed is the peak value of the number distribution ± 1 standard deviation of the distribution (obtained from DLS).

The peak value of the distribution was almost constant in the temperature range between 25 and 35 °C, with a small increase at 40 °C and a more significant change (+78% compared to the starting value) at 45 °C. The standard deviation also increased, meaning that a broader particle distribution was obtained, indicating formation of micellar aggregates at higher temperatures.[67] However, these results do show that this polymer could prove to be an interesting drug delivery vehicle since the average micellar size is still below 30 nm at body temperatures.

3.2.3 C6 incorporation

Coumarin-6 (C6) is a highly hydrophobic fluorescent dye that can be used to model the behaviour of lipophilic drugs for studies involving drug delivery and drug release.[78] For this reason, C6-loaded nanoparticles were prepared through nanoprecipitation. The MPEG-PHAz-MPEG copolymers were compared to Tween 20 and Pluronic L121, two commercially available amphiphilic copolymers used for stabilisation and encapsulation of hydrophobic molecules.[2, 79-83] Visual observation of filtered C6-loaded nanoparticle dispersions (plus a control sample of water without copolymer) gave a direct insight into the ability of some of the synthesised copolymers for encapsulating and stabilising C6 in water (Figure 7).

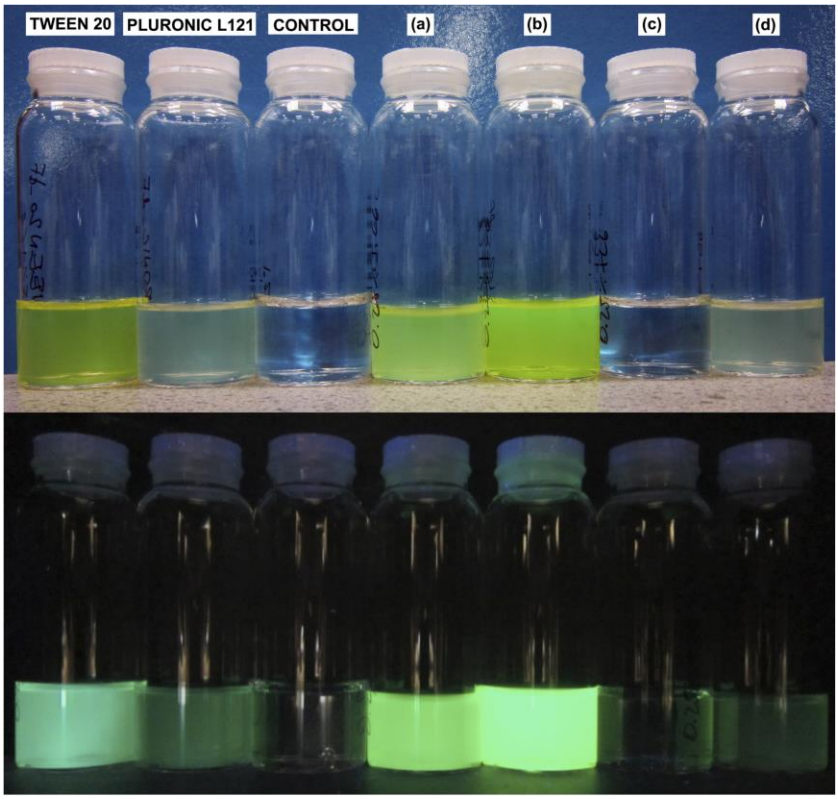

Figure 7 - Picture of the formulations for the synthesised copolymers (a) $MPEG_{12}$-$PHAz_3$-$MPEG_{12}$, (b) $MPEG_{12}$-$PHAz_6$-$MPEG_{12}$, (c) $MPEG_7$-$PHAz_3$-$MPEG_7$, (d) $MPEG_7$-$PHAz_3$-$MPEG_7$ compared to Tween 20 and Pluronic L121 under normal light (upper) and UV light (lower; λ=365 nm). No polymer was used in the control vial.

At first glance, it is clear that the MPEG-PHAz-MPEG polymers with longer hydrophilic segments (*i.e.* (a) $MPEG_{12}$-$PHAz_3$-$MPEG_{12}$ and (b) $MPEG_{12}$-$PHAz_6$-$MPEG_{12}$) were able to disperse the highest amount of C6 in the polar medium, with the latter displaying the strongest emission under UV light. The amount of C6 stabilised and dispersed in water was quantified through UV-Vis

analyses, by diluting small aliquots of these aqueous dispersions in THF and comparing the results with known C6 concentrations (Figure 8).

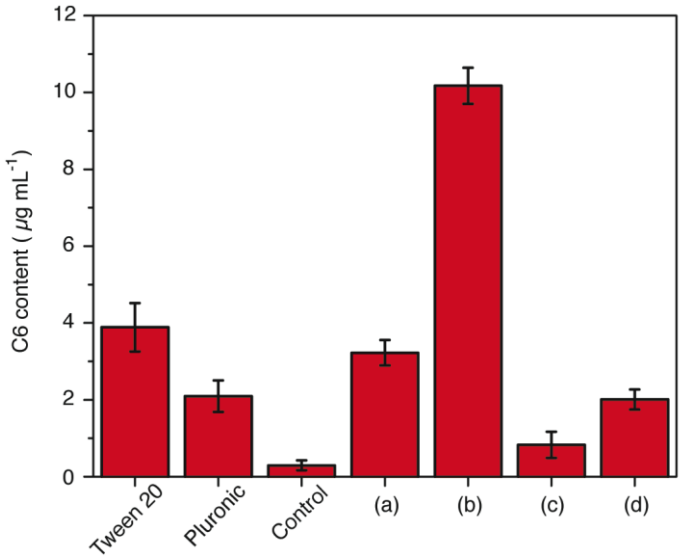

Figure 8 - C6 dispersed in the different formulations (μg of dye per mL of water). The synthesised copolymers (a) $MPEG_{12}$-$PHAz_3$-$MPEG_{12}$, (b) $MPEG_{12}$-$PHAz_6$-$MPEG_{12}$, (c) $MPEG_7$-$PHAz_3$-$MPEG_7$, (d) $MPEG_7$-$PHAz_3$-$MPEG_7$ are compared to Tween 20 and Pluronic L121. No polymer was used in the control sample. The copolymer (b) $MPEG_{12}$-$PHAz_6$-$MPEG_{12}$ showed the highest amount of C6 encapsulated and dispersed in water.

The UV-Vis results confirmed the visual observations and showed that the copolymer (a) had loading comparable to Tween 20 since around 3 μg mL^{-1} of dye were dispersed in water, whilst the copolymer (b) showed the highest loading with more than 10 μg mL^{-1} dispersed in water: three times higher than commercial Tween 20 and around 35 times the measured native solubility of C6 in H_2O (0.29 μg mL^{-1}). These data could be attributed to the different packing of the micellar core in the small micelles formed by this polymer. Furthermore, all of the dispersions were passed through 0.22 μm syringe filters to eliminate undissolved C6 and mimic the clearance by the RES,[75] so it is possible that some of the particles in the other formulations could have been removed during this step.

However, these preliminary results clearly demonstrate the ability of amphiphilic copolymers based on azelaic acid and 1,6-hexanediol to act as potential drug delivery vehicles.

3.2.4 CAC determination

Incorporation of the hydrophobic dye 1,6-diphenyl-1,3,5-hexatriene (DPH) was used to obtain the CAC of the copolymers. DPH is highly lipophilic and has a significantly lower intensity of

absorption at 330-380 nm in water compared with that in a lipophilic system. Thus as micelles or vesicles form, the dye is preferentially partitioned in the hydrophobic regions, leading to increased absorption.[6, 67] The dramatic change in absorbance gives information on the polymeric nanostructure formation and, hence, the CAC. As an example, the UV-Vis spectra obtained for the copolymer (b) $MPEG_{12}$-$PHAz_6$-$MPEG_{12}$ and the extrapolation of its CAC from the absorbance at 362 nm are shown (Figure 9).

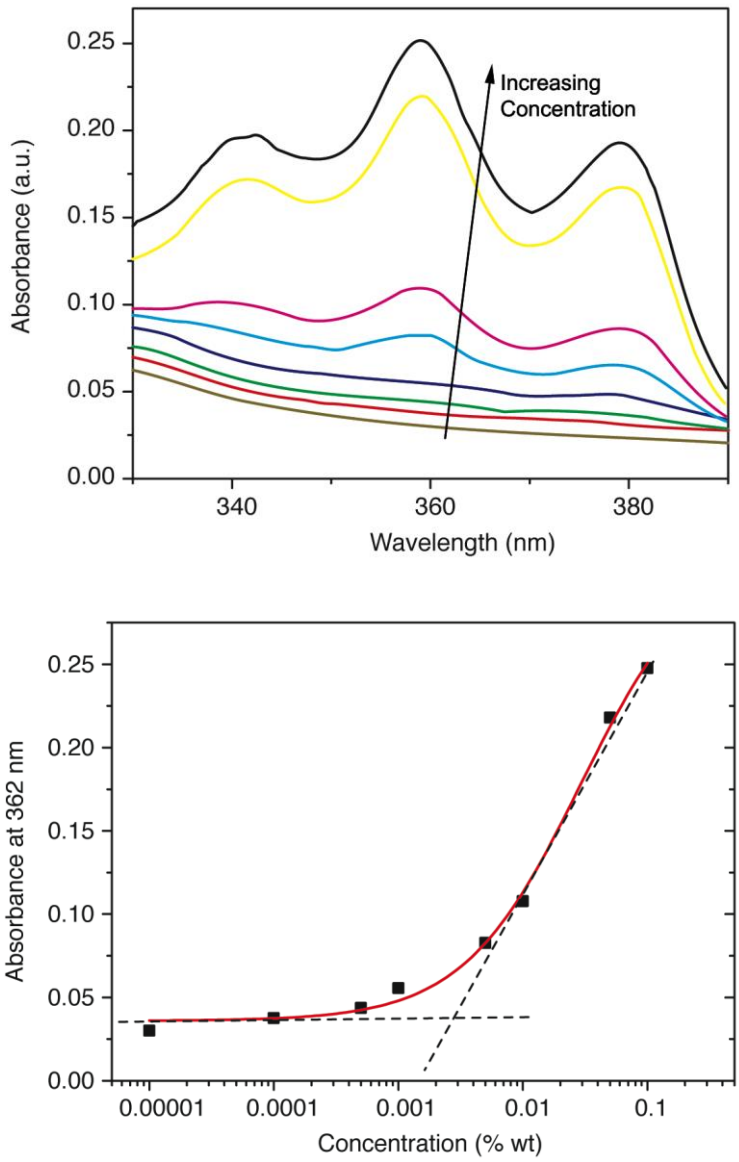

Figure 9 – CAC analysis of copolymer (b) $MPEG_{12}$-$PHAz_6$-$MPEG_{12}$ at 25 °C. The absorbance between 330 and 390 nm increases dramatically with polymer concentration (0.00001, 0.0001, 0.0005, 0.001, 0.005, 0.01, 0.05, 0.1% wt) at a fixed DPH concentration (0.004 mM) (upper). The CAC was determined by extrapolated lines (black dotted lines at high and low concentrations) of the absorbance maximum at 362 nm on the lower graph (data were fitted to a logistic growth function, red solid line, R^2>0.98).

The CAC of the copolymer (b) $MPEG_{12}$-$PHAz_6$-$MPEG_{12}$ was 0.0027% (27 µg mL^{-1}). The same analysis was conducted for the other copolymers to obtain their CAC (Table 4). The absorbance at 362 nm *vs* concentration for these copolymers is available in the SI.

Table 4 – CAC of the synthesised MPEG-PHAz-MPEG copolymers calculated from UV-Vis by the extrapolated lines of the absorbance maximum at 362 nm.

Product	*CAC*[a]		
	% wt	µg mL^{-1}	µM[b]
(a) $MPEG_{12}$-$PHAz_3$-$MPEG_{12}$	0.0047	47	18.8
(b) $MPEG_{12}$-$PHAz_6$-$MPEG_{12}$	0.0027	27	9.0
(c) $MPEG_7$-$PHAz_3$-$MPEG_7$	0.0021	21	11.7
(d) $MPEG_7$-$PHAz_6$-$MPEG_7$	0.0009	9	3.3

[a]The CAC error for each copolymer was less than 2%;
[b]Calculated from M_n^{NMR}

As expected, the copolymers containing the smallest hydrophilic segments (*i.e.* (c) and (d)) displayed the lowest CAC expressed in µg mL^{-1}. On the other hand, taking into account the molar mass of the copolymers, (b) and (d) displayed the lowest CAC expressed in µM (since these were characterised by the highest molecular weight). For a given length of MPEG block the copolymers containing the larger PHAz segment displayed a lower CAC values, as expected and already observed for similar systems elsewhere.[22, 73] Moreover, the CAC values determined for the copolymers (b), (c) and (d) are comparable to those of other copolymers currently used for drug delivery,[1, 10] and are much lower than the values observed for most of the Pluronics,[1, 3] other PEG-polyester-PEG amphiphilic copolymers described in literature[6, 67] and novel non ionic-biobased surfactants recently described elsewhere.[84] This is likely a result of the higher hydrophobicity of the PHAz block in combination with the packing of the polymer chains into crystalline regions, which also has been already shown to strongly influence CAC value.[75] These data clearly show that copolymers with azelaic acid and 1,6-hexanediol based backbones could be promising candidates for a new generation of renewable nano-carriers.

3.2.5 Surface tension reduction

Such amphiphilic polymers can also find applications in formulations for wetting agents, emulsifiers and detergents if there is a significant effect upon the surface tension.[13] We investigated

the reduction in surface tension through the maximum bubble pressure test and compared the values obtained to surface tension reduction achieved with commercial Tween 20 and Pluronic L121 (Figure 10).

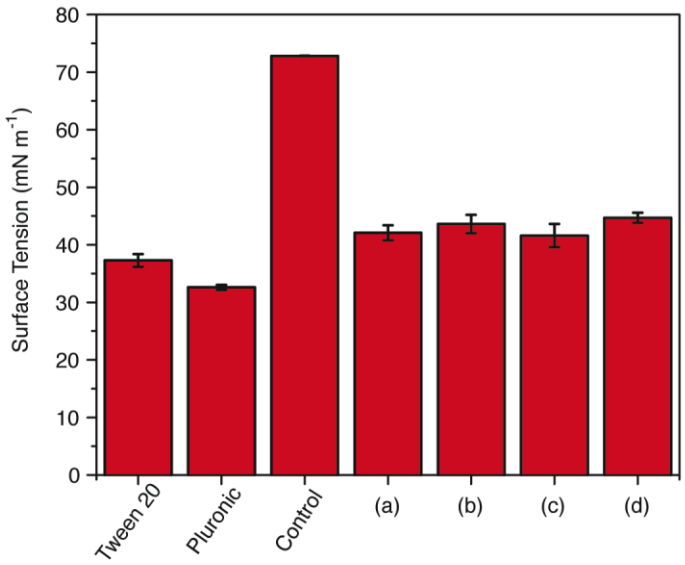

Figure 10 - Surface tension measured through maximum bubble pressure test. The synthesised copolymers (a) $MPEG_{12}$-$PHAz_3$-$MPEG_{12}$, (b) $MPEG_{12}$-$PHAz_6$-$MPEG_{12}$, (c) $MPEG_7$-$PHAz_3$-$MPEG_7$, (d) $MPEG_7$-$PHAz_3$-$MPEG_7$ are compared to Tween 20 and Pluronic L121 (0.2% wt in water). No polymer was used in the control sample. The MPEG-PHAz-MPEG copolymers showed a surface tension reduction comparable to those achieved by using commercial surfactants.

In current applications a molecule (or macromolecule) that is able to reduce the surface tension to below 60 mN m^{-1} is classed as a good surfactant.[12, 13] All the MPEG-PHAz-MPEG copolymers reduced the surface tension to around 40 mN m^{-1} and are comparable in their effects with Tween 20 and Pluronic L121, demonstrating that these novel materials could certainly provide interesting opportunities for formulations where a green biodegradable surfactant is required.

4 Conclusions

A novel low-temperature approach to enzymatic synthesis of polyesters in $scCO_2$ has been exploited to develop new amphiphilic block copolymers based on azelaic acid and 1,6-hexanediol as building blocks of the hydrophobic backbone. The polymerisations were carried out in a solvent-

free $scCO_2$ system, using natural enzyme CaLB as a catalyst at 35 °C and achieving remarkably high yields.

The structural and physical properties of the novel polymers have been confirmed by NMR, DSC and GPC showing that the synthetic route provides excellent control over the polymer molecular weight and properties.

DLS, TEM, NMR and UV-Vis studies were carried out to investigate the self-assembly of these polymers in water, obtaining promising preliminary data for nanostructures formation and encapsulation. Coumarin-6 loading tests demonstrated the ability of the polymers to disperse and stabilise lipophilic molecules in aqueous environment, and the CAC of these novel MPEG-PHAz-MPEG copolymers was determined by UV-Vis using 1,6-diphenyl-1,3,5-hexatriene as a probe to show high stability of the aggregated nanostructure.

Finally, the surface tension reduction achieved by dispersing these novel polymers in water was determined by maximum bubble pressure test and compared to those achieved for commercially available non-ionic polymeric surfactants. The results showed a significant reduction, indicating that these new azelaic acid based copolymers might find applications also as surfactants in detergents and body-care formulations. Further analyses need to be done to investigate the self-assembly of these copolymers in water more in-depth and to evaluate their real potential in drug delivery and other applications.

Acknowledgments

The research leading to these results has received funding from the People Programme (Marie Curie Actions) of the European Union's Seventh Framework Programme FP7/2007-2013/under REA grants agreement No. [289253].

We thank Richard Wilson, Pete Fields and Mark Guyler (University of Nottingham) for the technical input with the high-pressure equipment, Nicola Weston (University of Nottingham) for TEM acquisition, Amy Goddard (University of Nottingham/Croda International plc) for the surface tension tests, Shazad Aslam for NMR support and Dr Claudia Conte for sharing her expertise on micelles preparation and characterisation.

5 References

1. M.-C. Jones and J.-C. Leroux, *European Journal of Pharmaceutics and Biopharmaceutics*, 1999, **48**, 101-111.
2. G. Riess, *Progress in Polymer Science*, 2003, **28**, 1107-1170.
3. Z. Ahmad, A. Shah, M. Siddiq and H.-B. Kraatz, *RSC Advances*, 2014, **4**, 17028.
4. S. Payyappilly, S. Dhara and S. Chattopadhyay, *Journal of biomedical materials research. Part A*, 2014, **102**, 1500-1509.
5. K. K. Bansal, D. Kakde, L. Purdie, D. J. Irvine, S. M. Howdle, G. Mantovani and C. Alexander, *Polym. Chem.*, 2015, **6**, 7196-7210.
6. M. J. Hwang, J. M. Suh, Y. H. Bae, S. W. Kim and B. Jeong, *Biomacromolecules*, 2005, **6**, 885-890.
7. C. Gong, S. Shi, L. Wu, M. Gou, Q. Yin, Q. Guo, P. Dong, F. Zhang, F. Luo, X. Zhao, Y. Wei and Z. Qian, *Acta biomaterialia*, 2009, **5**, 3358-3370.
8. C. Y. Gong, P. W. Dong, S. Shi, S. Z. Fu, J. L. Yang, G. Guo, X. Zhao, Y. Q. Wei and Z. Y. Qian, *J Pharm Sci*, 2009, **98**, 3707-3717.
9. Z. L. Tyrrell, Y. Shen and M. Radosz, *Progress in Polymer Science*, 2010, **35**, 1128-1143.
10. W. Xu, P. Ling and T. Zhang, *Journal of drug delivery*, 2013, **2013**, 340315.
11. G. Bonacucina, M. Cespi, G. Mencarelli, G. Giorgioni and G. F. Palmieri, *Polymers*, 2011, **3**, 779-811.
12. J. Texter, *Reactions And Synthesis In Surfactant Systems*, Taylor & Francis, 2001.
13. R. J. Farn, *Chemistry and Technology of Surfactants*, Wiley, 2008.
14. J. S. Lee and J. Feijen, *Journal of Controlled Release*, 2012, **161**, 473-483.
15. R. Z. Xiao, Z. W. Zeng, G. L. Zhou, J. J. Wang, F. Z. Li and A. M. Wang, *International journal of nanomedicine*, 2010, **5**, 1057-1065.
16. R. Ooms, M. Dusselier, J. A. Geboers, B. Op de Beeck, R. Verhaeven, E. Gobechiya, J. A. Martens, A. Redl and B. F. Sels, *Green Chem.*, 2014, **16**, 695-707.
17. J. Pang, M. Zheng, R. Sun, A. Wang, X. Wang and T. Zhang, *Green Chemistry*, 2015, DOI: 10.1039/C5GC01771H.
18. J. Chen, S. K. Spear, J. G. Huddleston and R. D. Rogers, *Green Chemistry*, 2005, **7**, 64-82.
19. A. G. West, C. Barner-Kowollik and S. Perrier, *Polymer*, 2010, **51**, 3836-3842.
20. R. Marchal, E. Nicolau, J. P. Ballaguet and F. Bertoncini, *International Biodeterioration & Biodegradation*, 2008, **62**, 384-390.
21. C. Gong, S. Shi, P. Dong, B. Kan, M. Gou, X. Wang, X. Li, F. Luo, X. Zhao, Y. Wei and Z. Qian, *International journal of pharmaceutics*, 2009, **365**, 89-99.
22. L. Piao, Z. Dai, M. Deng, X. Chen and X. Jing, *Polymer*, 2003, **44**, 2025-2031.
23. A. Gandini, *Macromolecules*, 2008, **41**, 9491-9504.
24. M. N. Belgacem and A. Gandini, *Monomers, Polymers and Composites from Renewable Resources*, Elsevier Science, 2011.
25. M. F. Kemmere and T. Meyer, *Supercritical carbon dioxide in polymer reaction engineering / edited by Maartje F. Kemmere and Thierry Meyer*, Wiley-VCH, 2005.
26. C. Tsioptsias, M. K. Paraskevopoulos, D. Christofilos, P. Andrieux and C. Panayiotou, *Polymer*, 2011, **52**, 2819-2838.
27. C. Gutiérrez, M. T. Garcia, S. Curia, S. M. Howdle and J. F. Rodriguez, *The Journal of Supercritical Fluids*, 2014, **88**, 26-37.
28. F. Picchioni, *Polymer International*, 2014, **63**, 1364-1399.
29. J. Jennings, M. Beija, J. T. Kennon, H. Willcock, R. K. O'Reilly, S. Rimmer and S. M. Howdle, *Macromolecules*, 2013, **46**, 6843-6851.
30. L. Du, J. Y. Kelly, G. W. Roberts and J. M. DeSimone, *The Journal of Supercritical Fluids*, 2009, **47**, 447-457.

31. J. Jennings, M. Beija, A. P. Richez, S. D. Cooper, P. E. Mignot, K. J. Thurecht, K. S. Jack and S. M. Howdle, *Journal of the American Chemical Society*, 2012, **134**, 4772-4781.
32. I. Tsivintzelis, E. Pavlidou and C. Panayiotou, *The Journal of Supercritical Fluids*, 2007, **42**, 265-272.
33. B. Bungert, G. Sadowski and W. Arlt, *Fluid Phase Equilibria*, 1997, **139**, 349-359.
34. S. P. Nalawade, F. Picchioni and L. P. B. M. Janssen, *Chemical Engineering Science*, 2007, **62**, 1712-1720.
35. C. A. Kelly, A. Naylor, L. Illum, K. M. Shakesheff and S. M. Howdle, *Advanced Functional Materials*, 2012, **22**, 1684-1691.
36. S. M. Howdle, M. S. Watson, M. J. Whitaker, M. C. Davies, K. M. Shakesheff, V. K. Popov, F. S. Mandel and J. D. Wang, *Chemical Communications*, 2001, 109-110.
37. Z. Zhang and Y. P. Handa, *Macromolecules*, 1997, **30**, 8505-8507.
38. D. Gourgouillon, H. M. N. T. Avelino, J. M. N. A. Fareleira and M. Nunes da Ponte, *The Journal of Supercritical Fluids*, 1998, **13**, 177-185.
39. Z. Zhang and Y. P. Handa, *Journal of Polymer Science Part B: Polymer Physics*, 1998, **36**, 977-983.
40. S. Curia, D. S. A. De Focatiis and S. M. Howdle, *Polymer*, 2015, **69**, 17-24.
41. P. Dubois, O. Coulembier and J. M. Raquez, *Handbook of Ring-Opening Polymerization*, Wiley, 2009.
42. G. Montaudo and P. Rizzarelli, *Polymer Degradation and Stability*, 2000, **70**, 305-314.
43. D. N. Bikiaris, G. Z. Papageorgiou and D. S. Achilias, *Polymer Degradation and Stability*, 2006, **91**, 31-43.
44. G. Z. Papageorgiou and D. N. Bikiaris, *Biomacromolecules*, 2007, **8**, 2437-2449.
45. G. Z. Papageorgiou, D. N. Bikiaris, D. S. Achilias, S. Nanaki and N. Karagiannidis, *Journal of Polymer Science Part B: Polymer Physics*, 2010, **48**, 672-686.
46. F. J. C. Roe, E. Boyland and K. Millican, *Food and Cosmetics Toxicology*, 1965, **3**, 277-280.
47. A. P. de Groot, V. J. Feron and H. P. Til, *Food and Cosmetics Toxicology*, 1973, **11**, 19-30.
48. J. Zhang, H. Shi, D. Wu, Z. Xing, A. Zhang, Y. Yang and Q. Li, *Process Biochemistry*, 2014, **49**, 797-806.
49. Y. Poojari and S. J. Clarson, *Biocatalysis and Agricultural Biotechnology*, 2013, **2**, 7-11.
50. A. Pellis, L. Corici, L. Sinigoi, N. D'Amelio, D. Fattor, V. Ferrario, C. Ebert and L. Gardossi, *Green Chemistry*, 2015, **17**, 1756-1766.
51. S. Curia, A. F. Barclay, S. Torron, M. Johansson and S. M. Howdle, *Philosophical Transactions of the Royal Society of London A: Mathematical, Physical and Engineering Sciences*, 2015, **373**, 1-16.
52. C. A. Cherrington, M. Hinton, G. C. Mead and I. Chopra, in *Advances in Microbial Physiology*, eds. A. H. Rose and D. W. Tempest, Academic Press, 1991, vol. Volume 32, pp. 87-108.
53. S. Maddin, *Journal of the American Academy of Dermatology*, 1999, **40**, 961-965.
54. D. L. Sparks, R. Hernandez, L. A. Estévez, N. Meyer and T. French, *Journal of Chemical & Engineering Data*, 2007, **52**, 1246-1249.
55. J. Sun Yu and A. Keun Kim, *J Biomed Sci*, 2010, **17**, 1-5.
56. H. J. Arpe, *Ullmann's Encyclopedia of Industrial Chemistry, Ullmann's Encyclopedia of Industrial Chemistry: Set: Printed Fifth Edition plus Sixth Edition Electronic Release*, Wiley, 1999.
57. G. Z. Papageorgiou, D. N. Bikiaris, D. S. Achilias and N. Karagiannidis, *Macromolecular Chemistry and Physics*, 2010, **211**, 2585-2595.
58. G. Z. Papageorgiou, D. N. Bikiaris, D. S. Achilias, E. Papastergiadis and A. Docoslis, *Thermochimica Acta*, 2011, **515**, 13-23.
59. *US Pat.*, WO2013101969 A1, 2013.

60. J. Tuteja, H. Choudhary, S. Nishimura and K. Ebitani, *ChemSusChem*, 2014, **7**, 96-100.
61. *US Pat.*, WO2015027184 A1, 2015.
62. F. C. Loeker, C. J. Duxbury, R. Kumar, W. Gao, R. A. Gross and S. M. Howdle, *Macromolecules*, 2004, **37**, 2450-2453.
63. M. Eriksson, L. Fogelström, K. Hult, E. Malmström, M. Johansson, S. Trey and M. Martinelle, *Biomacromolecules*, 2009, **10**, 3108-3113.
64. M. Eriksson, K. Hult, E. Malmström, M. Johansson, S. M. Trey and M. Martinelle, *Polymer Chemistry*, 2011, **2**, 714-719.
65. S. Torron and M. Johansson, *Journal of Polymer Science Part A: Polymer Chemistry*, 2015, **53**, 2258-2266.
66. H. E. Gottlieb, V. Kotlyar and A. Nudelman, *The Journal of Organic Chemistry*, 1997, **62**, 7512.
67. B. Jeong, Y. Han Bae and S. Wan Kim, *Colloids and Surfaces B: Biointerfaces*, 1999, **16**, 185-193.
68. L. Gustini, B. A. J. Noordover, C. Gehrels, C. Dietz and C. E. Koning, *European Polymer Journal*, 2015, **67**, 459-475.
69. A. Noshay and J. E. McGrath, *Block Copolymers: Overview and Critical Survey*, Elsevier Science, 2013.
70. J. Mark, *Physical Properties of Polymers*, Cambridge University Press, 2004.
71. Y. Huang, X. Xu, X. Luo and D. Ma, *Chinese Journal of Polymer Science*, 2002, **20**, 45-51.
72. X. Kong, H. Qi and J. M. Curtis, *Journal of Applied Polymer Science*, 2014, **131**, 1-9.
73. Y.-C. Wang, L.-Y. Tang, T.-M. Sun, C.-H. Li, M.-H. Xiong and J. Wang, *Biomacromolecules*, 2008, **9**, 388-395.
74. L. Zhang and A. Eisenberg, *Journal of the American Chemical Society*, 1996, **118**, 3168-3181.
75. L. Glavas, P. Olsen, K. Odelius and A. C. Albertsson, *Biomacromolecules*, 2013, **14**, 4150-4156.
76. G. Rizis, PhD PhD Thesis, McGill University, 2013.
77. S. C. Owen, D. P. Y. Chan and M. S. Shoichet, *Nano Today*, 2012, **7**, 53-65.
78. I. Rivolta, A. Panariti, B. Lettiero, S. Sesana, P. Gasco, M. R. Gasco, M. Masserini and G. Misserocchi, *Journal of Physiology and Pharmacology*, 2011, **62**, 45-53.
79. T.-F. Yang, C.-N. Chen, M.-C. Chen, C.-H. Lai, H.-F. Liang and H.-W. Sung, *Biomaterials*, 2007, **28**, 725-734.
80. M. Verbrugghe, P. Sabatino, E. Cocquyt, P. Saveyn, D. Sinnaeve, P. Van der Meeren and J. C. Martins, *Colloids and Surfaces A: Physicochemical and Engineering Aspects*, 2010, **372**, 28-34.
81. S. Kalepu, M. Manthina and V. Padavala, *Acta Pharmaceutica Sinica B*, 2013, **3**, 361-372.
82. I. Pepić, J. Lovrić, A. Hafner and J. Filipović-Grčić, *Drug Development and Industrial Pharmacy*, 2014, **40**, 944-951.
83. E. S. Lee, Y. T. Oh, Y. S. Youn, M. Nam, B. Park, J. Yun, J. H. Kim, H. T. Song and K. T. Oh, *Colloids and surfaces. B, Biointerfaces*, 2011, **82**, 190-195.
84. C. Gozlan, E. Deruer, M.-C. Duclos, V. Molinier, J.-M. Aubry, A. Redl, N. Duguet and M. Lemaire, *Green Chemistry*, 2016, DOI: 10.1039/c5gc02131f.